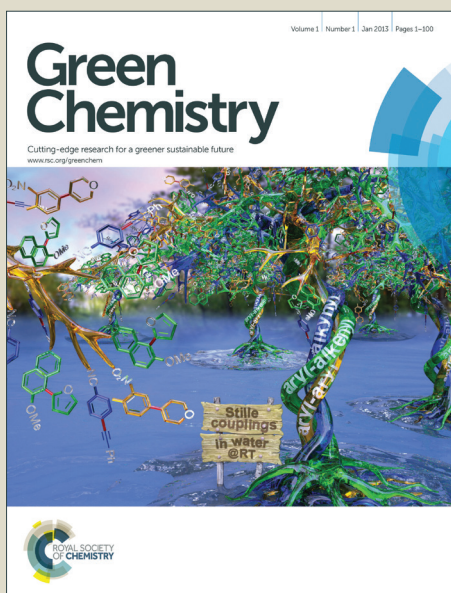


Green Chemistry

Accepted Manuscript



This is an *Accepted Manuscript*, which has been through the Royal Society of Chemistry peer review process and has been accepted for publication.

Accepted Manuscripts are published online shortly after acceptance, before technical editing, formatting and proof reading. Using this free service, authors can make their results available to the community, in citable form, before we publish the edited article. We will replace this *Accepted Manuscript* with the edited and formatted *Advance Article* as soon as it is available.

You can find more information about *Accepted Manuscripts* in the [Information for Authors](#).

Please note that technical editing may introduce minor changes to the text and/or graphics, which may alter content. The journal's standard [Terms & Conditions](#) and the [Ethical guidelines](#) still apply. In no event shall the Royal Society of Chemistry be held responsible for any errors or omissions in this *Accepted Manuscript* or any consequences arising from the use of any information it contains.



www.rsc.org/greenchem

ARTICLE

Fluoride-free synthesis of Sn-BEA catalyst by dry gel conversion

Cite this: DOI: 10.1039/x0xx00000x

Chun-Chih Chang, Hong Je Cho, Zhuopeng Wang, Xuanting Wang and Wei Fan*

Received 00th December 2014,
Accepted 00th December 2014

DOI: 10.1039/x0xx00000x

www.rsc.org/

Sn containing molecular sieve with BEA topology (Sn-BEA) is an active Lewis catalyst for a large variety of redox reactions. However, the synthesis of Sn-BEA often requires the use of toxic chemicals (e.g. hydrofluoric acid). In the study, we demonstrated that an active Sn-BEA catalyst can be directly synthesized from a non-fluoride medium *via* a dry gel conversion method with the aid of seed crystals. It was shown that seeding of zeolite BEA crystals can facilitate crystal growth and lead to BEA topology with framework Sn. Furthermore, it was found that ion-exchange with ammonium ion is indispensable to retain the crystal structure during calcination. The catalytic activity of the Sn-BEA catalyst was evaluated by the isomerization of glucose and reaction of pyruvaldehyde in aqueous phase, and compared to the conventional hydrophobic Sn-BEA synthesized from a fluoride medium. The catalytic activity of the Sn-BEA synthesized in the absence of fluoride was found to be lower than that of the conventional Sn-BEA for catalyzing the isomerization of glucose in aqueous phase, which could be attributed to its hydrophilic surface. For the reaction of pyruvaldehyde in aqueous phase, the Sn-BEA synthesized in this study showed similar activity with the conventional hydrophobic Sn-BEA, indicating the catalytic activity of Sn-BEA catalysts largely depends on the type of reactions. The current work provides the first example of direct preparation of Sn-BEA catalyst in a caustic medium.

Introduction

Zeolites have been extensively used in catalysis, ion-exchange and separation due to their highly crystalline microporous structure and a large variety of available frameworks and compositions.¹⁻⁴ In addition to Brønsted acid catalysts, molecular sieves containing tetrahedrally coordinated Sn, Ti and Zr have been used for Lewis acid-catalyzed redox reactions.⁵⁻¹¹ In particular, Sn-BEA molecular sieve, a crystalline stannosilicate with BEA topology, exhibits extraordinary Lewis acidity for selectively activating functional groups of organic molecules involved in fine chemical syntheses.¹²⁻¹⁸ The catalyst has shown promising activity for the catalytic oxidation of saturated and unsaturated ketones through the Baeyer-Villiger reaction and the reduction of carbonyl compounds with secondary alcohols through the Meerwein-Ponndorf-Verley reaction.^{9, 10, 19} Moreover, Moliner *et al.* recently reported that Sn-BEA is water-tolerant and capable of catalyzing isomerization of glucose to fructose in aqueous phase,⁷ a key intermediate step for the conversion of biomass into chemicals and fuels.²⁰ Similarly, Sn-BEA has also been used to catalyze the isomerization of pentose and triose sugars to form xylulose, methyl lactate and lactic acid.^{6, 8, 21} The outstanding Lewis acidity of Sn-BEA catalyst in aqueous phase is likely due to the hydrophobic environment created by the defect-free siliceous surface.^{15, 22, 23}

Although Sn containing molecular sieve shows intriguing catalytic properties, typical synthesis of Sn-BEA involves the

utilization of toxic hydrofluoric acid and lengthy synthesis time (up to 40 days),^{7, 10, 24} leading to several environmental and practical concerns. Significant efforts have been made to improve the synthesis process of Sn-BEA, such as using less toxic chemicals²⁵ and shortening crystallization time by seeded growth method.²⁶ However, fluoride medium was still used in all syntheses. Although more benign chemicals such as ammonium fluoride (NH₄F) and sodium fluoride (NaF) can be potentially used in the synthesis, non-fluoride method is still strongly desired due to potential health risk related to chronic excessive exposure to fluorides.²⁷ Recently, post-synthesis approaches have been used to synthesize Sn-BEA in the absence of fluorides. For instance, Li *et al.* reported that Sn can be grafted onto dealuminated zeolite BEA by chemical vapor deposition using tin (IV) chloride vapor; Hammond *et al.* proposed a solid state ion exchange method *via* mixing tin (II) acetate with dealuminated zeolite BEA; Dijkmans *et al.* utilized a solution-based method to insert Sn into dealuminated zeolite BEA.²⁸⁻³⁰ In all post-synthesis methods, Sn was incorporated into the defects generated by the dealumination process. Condensation of various Sn sources with silanol defects resulted in the formation of tetrahedrally coordinated Sn sites. Sn concentration in the samples can be easily tailored by controlling the amount of Sn source applied in the treatment. The materials made from the post-synthesis approaches show interesting catalytic performances in Baeyer-Villiger oxidation, isomerization of triose sugar (such as dihydroxyacetone to lactates in alcohols) and glucose. However, due to the low

mobility of Sn sources used in the syntheses and the lack of ability to control the type and amount of defects generated by the dealumination process, it is a challenge to completely diminish all defects in the dealuminated zeolites by the incorporation of framework Sn. This is likely one of the reasons why very different catalytic activity was observed for the Sn-BEA catalysts made by the post-synthesis methods.

To our best knowledge, direct synthesis of Sn-BEA catalyst from a fluoride-free system has not been achieved so far. The challenges are mainly due to the difficulties in the crystallization of siliceous zeolite BEA in the absence of fluoride and incorporation of tetrahedrally coordinated Sn in zeolite frameworks. It has been known that during zeolite syntheses fluoride can facilitate the mineralization of silica sources and compensate the positive charges associated with the organic structure directing agents (OSDAs) employed in the syntheses.³¹ As a result, the zeolites synthesized in the presence of fluoride exhibit fewer defects and higher crystallinity than the ones made under conventional hydrothermal synthesis conditions. In order to synthesize high silica or siliceous zeolites without using fluoride, the positive charges of OSDA must be compensated by the defects located in the framework (e.g. $\equiv\text{Si-O}^-\cdots\text{HO-Si}\equiv$), which is particularly challenging for relative small OSDAs, such as tetraethylammonium (TEA) used in zeolite BEA synthesis. The small OSDAs usually result in an increased number of OSDAs occluded in zeolite channels (e.g. 6 TEA/unit cell for BEA, while only 4 TPA/unit cell for MFI),^{32, 33} which requires more defects for charge compensation and could compete with the formation of stable crystalline phases. This challenge has been partially solved by using dry gel conversion (DGC) method that was initially developed for ZSM-5 zeolite and later extended to several other zeolites including high silica zeolite BEA.^{34, 35} In the DGC method, crystallization of a concentrated gel is carried out under saturated steam generated from liquid water which is not allowed to directly contact with the synthesis gel. Using this method, zeolite BEA with a wide range of Si/Al ratio has been successfully synthesized.³⁵ Although incorporation of other heteroatoms in zeolite frameworks by the DGC method has also been demonstrated for TS-1 and Ti-BEA,^{36, 37} synthesis of Sn-BEA by the DGC method has not succeeded, likely due to the relatively large atomic size of Sn (Ti^{4+} : 0.68 Å, Sn^{4+} : 0.71 Å) and the incomparable hydrolysis rate of Sn source with silica source. These differences could lead to an amorphous phase, incredible slow crystallization and non-framework Sn as shown later in this study.

Herein, a direct and fluoride-free synthesis route is developed for Sn-BEA. We demonstrated that an active Sn-BEA catalyst can be directly synthesized by the DGC method without using any fluoride containing chemicals. The use of crystalline seeds and inorganic cations for charge compensation is essential for the crystallization of Sn-BEA in the absence of fluoride. The inorganic cations in the as-synthesized sample must be ion-exchanged to ammonium type in order to maintain the crystalline structure of the formed catalysts during calcination. The synthesized Sn-BEA exhibits hydrophilic nature compared to the ones synthesized in the presence of fluoride.

Experimental

Synthesis of Sn-BEA by the DGC method

A dry gel conversion method was used to synthesize Sn-BEA in the absence of fluoride. In a typical synthesis, 0.0448 g of sodium hydroxide (NaOH, Fisher) was dissolved in 3.09 g of 35 wt% tetraethylammonium hydroxide (TEAOH, Alfa Aesar or ZeoGen SDA 440, SACHEM) solution and 14 g of deionized water in a plastic vessel followed by adding 1 g of fumed silica (Cab-O-Sil M5, Cabot). The obtained solution was magnetically stirred for 1 h at room temperature. Tin source solution containing 0.0548 g of tin tert-butoxide ($\text{Sn}(\text{OC}_4\text{H}_9)_4$, Aldrich) and 0.254 mL of 30% hydrogen peroxide aqueous solution (H_2O_2 , Fisher) was mixed for 1 h prior to adding into the solution prepared previously. The resulting solution was stirred for 2 h at room temperature. A dealuminated zeolite BEA seed solution (4 wt% with respect to fumed silica added, particle size of the seed is around 200 nm) was then added, and the solvent in the translucent mixture was evaporated at 80 °C with stirring in an oil bath for 24 h, leading to a dry gel. Detailed synthesis procedure for the dealuminated zeolite BEA seed solution is available in our previous work.²⁶ The final composition of the dry gel is SiO_2 : 0.008 SnO_2 : 0.22 TEA_2O : 0.034 Na_2O . Other cations were also employed in the synthesis, including potassium hydroxide (KOH, Fisher), lithium hydroxide (LiOH, Alfa Aesar), ammonium nitrate (NH_4NO_3 , Alfa Aesar), ammonium hydrogen carbonate (NH_4HCO_3 , Alfa Aesar) and ammonium hydroxide (NH_4OH , Fisher). The obtained dry gel (ca. 2 g) was ground into powder and put into a Teflon-lined stainless steel autoclave with a cup volume of ca. 50 mL. A portion of 0.5 mL of deionized water was added into the autoclave in a separate Teflon cup to avoid direct contact between the dry gel and water. The autoclave was then placed in an oven preheated to 140 °C for crystallization. The as-made sample was washed by filtration with 1 L of deionized water and dried at 100 °C overnight (denoted as Sn-BEA-AM). Ion-exchange was carried out by treating 0.25 g of as-made zeolites with 25 mL of 1 M ammonium nitrate (NH_4NO_3 , J. T. Baker) solution for 2 h at 80 °C. The process was repeated five times. Removal of OSDA and ammonium ions was obtained by calcining the powder in a muffle furnace at 550 °C for 12 h with a ramping rate of 1 °C min^{-1} (denoted as Sn-BEA-IE). Synthesis of Sn-BEA (denoted as Sn-BEA-F, Si/Sn = 125) from a fluoride medium was achieved by using a method reported in our previous study.²⁶ Extra-framework SnO_2 in siliceous zeolite BEA sample ($\text{SnO}_2/\text{Si-BEA}$, Si/Sn=125) were prepared according to literature.³⁸ Detailed procedures are available in Supplementary Information.

Characterizations

Samples were characterized by X-ray diffraction (XRD), scanning electron microscopy (SEM), transmission electron microscopy (TEM), nitrogen sorption measurements, thermogravimetric analysis (TGA), diffuse reflectance ultraviolet-visible spectroscopy (DR UV-Vis), FT-IR spectroscopy and inductively coupled plasma mass spectroscopy (ICP-MS). XRD measurements were performed on a diffractometer (X'Pert Pro, PANalytical) using Cu K α radiation generated at 45 kV and 40 mA from 2 theta of 4° to

40° with a step size of 0.02°. SEM was performed on a Magellan 400 (FEI) with an accelerating voltage of 3.0 kV, and the samples were coated with platinum/palladium alloy prior to observation. TEM images were recorded on a Joel JEM-2000FX (200 kV). Nitrogen adsorption-desorption isotherms were collected on an automated gas sorption analyzer (Autosorb iQ₂, Quantachrome) at 77 K. The samples were outgassed at 300 °C for 12 h under vacuum before measurement. The thermogravimetric analysis (TGA) was performed on a thermogravimetric analyzer (SDT600, TA) with a ramping rate of 10 °C min⁻¹ under helium flow. Prior to the analysis, samples are contacted with liquid water and dried in a convection oven at 70 °C overnight. DR UV-Vis measurements were done on a Cary 50 spectrometer with a diffuse reflectance attachment. Barium sulphate was used as a background material. FT-IR experiment was carried out using a Praying Mantis™ DRIFT accessory (Harrick) in a high-temperature reaction cell (Harrick) allowing controls of atmosphere, temperature and adsorption of probe molecules over the zeolite samples. The samples were pretreated with helium flow at 550 °C for 1 h prior to adsorption (pyridine or deuterated acetonitrile). For FT-IR measurements of samples with adsorbed pyridine, pyridine (Alfa Aesar) vapor was carried by helium and in contact with the samples at 120 °C for 10 min. After heating up to 250 °C for 1 h to desorb weakly adsorbed pyridine, the spectrum was recorded on a FT-IR spectrometer (Equinox 55, Bruker) equipped with MCT detector with a resolution of 2 cm⁻¹ at 120 °C. For deuterated acetonitrile (CD₃CN, Aldrich) adsorption, it was adsorbed on the samples at 30 °C followed by flowing helium for 30 min. CD₃CN was then desorbed at 100 °C for various periods of time. The spectra were acquired at 30 °C and normalized with the Si-O-Si overtones at 1800-2000 cm⁻¹. Potassium bromide (KBr, Acros) was used as background in this case. Elemental analysis was carried out in the Analytical Geochemistry Lab, Dept. of Earth Sciences in University of Minnesota using an inductively coupled plasma mass spectrometer (ICP-MS, Thermo Scientific XSERIES 2).

Catalytic activity tests

The catalytic activity of the obtained Sn-BEA catalysts was studied for sugar isomerization including the conversion of glucose into fructose and conversion of pyruvaldehyde (PA) into lactic acid (LA) in water. For glucose isomerization, 0.8 g of 10 wt% of aqueous glucose (Acros) solution was mixed with 0.068 g of catalyst in a closed glass vial. After the reaction mixture was heated at 95 °C for 15 min on an aluminum heating block, it was cooled down in ice water and filtered with a 0.2 μm syringe filter. Conversion of PA in water was carried out with 0.056 g of PA solution (40 wt% in water, Aldrich) in 1 g of water with 0.02 g of catalyst at 70 °C for 15 min. The filtrate was then analyzed on a HPLC system (LC-20C Shimadzu) equipped with a refractive index (RI) detector. Separation of sugar isomers was done by running the sample through an HPX-87H proton type column (BioRad) at 30 °C under a flow rate of 0.6 mL min⁻¹ with 0.005 M sulphuric acid

(H₂SO₄, Fisher). Turnover frequencies (TOF) of the catalysts were calculated based on the product formation with a unit of min⁻¹ on each Sn site (the moles of Sn site is obtained from elemental analysis):

$$TOF (min^{-1}) = \frac{(\text{moles of product formed})}{(\text{moles of Sn in the catalyst}) * (\text{reaction time})}$$

Results and Discussion

Synthesis parameters for Sn-BEA by the DGC method

Synthesis of Sn-BEA by the DGC method was first performed with or without adding zeolite BEA seeds. As shown in Fig. 1, characteristic XRD peaks corresponding to the BEA topology are observed for the sample synthesized with adding zeolite BEA seeds after 5 days of crystallization, revealing that highly crystalline BEA zeolite has been synthesized without any impurity phase. Crystallization is apparently slow in the absence of zeolite seeds, and an unidentifiable reflection peak dominates the spectrum after 5 days of crystallization. Longer crystallization time (20 days) does not yield pure BEA phase. These results indicate that adding zeolite BEA seeds not only facilitates the crystallization but also directs the formation of desired crystal structure under the present synthesis conditions. Thus, it is concluded that the seeding approach plays an essential role in the crystallization of pure Sn-BEA phase from the dry gel. Zeolite seeds were used in all the syntheses in this study later.

It is also found that the use of alkali ions is crucial for the crystallization of Sn-BEA *via* the DGC method. As revealed in Fig. 2(a), when Na₂O/SiO₂ ratio in initial gel is lower than 0.034, the crystallinity of the obtained samples is significantly lower than the samples made with higher concentration of Na⁺ after 5 days of crystallization.

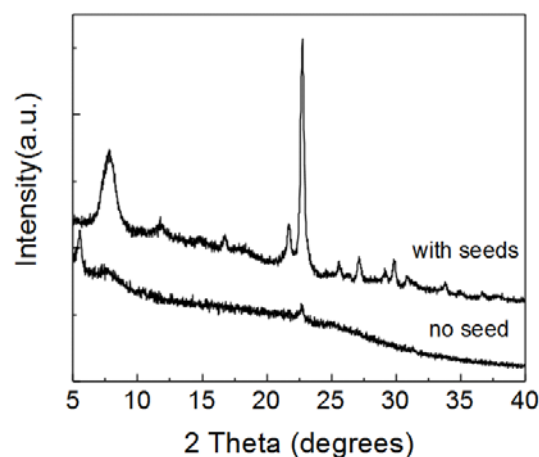


Fig. 1 XRD patterns of the samples prepared with and without using zeolite BEA seeds after dry gel conversion at 140 °C for 5 days

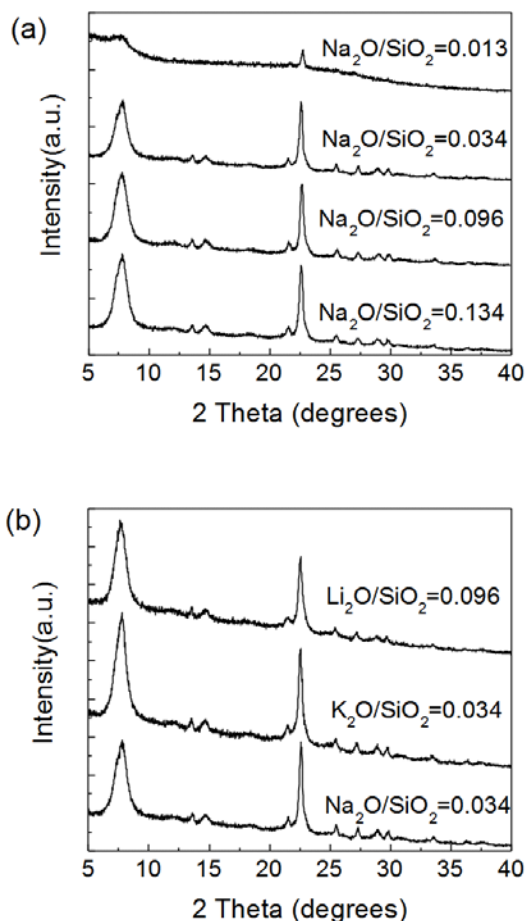


Fig. 2 XRD patterns of the samples synthesized with (a) different Na contents and (b) different alkali ions. The crystallization was carried out at 140 °C for 5 days, followed by ion-exchange and calcination.

Only very weak reflections can be observed in the samples when no alkali ion was added (Fig. S1), and the signals are likely attributed to the seed crystals present in the synthesis mixture. Different alkali ions (Li^+ and K^+) were also tested for the crystallization of Sn-BEA from the DGC method. The XRD patterns from the obtained samples suggest that zeolite BEA phase can be obtained in all cases (Fig. 2(b)). The result clearly indicates that the alkali ions do not affect the crystalline structure of formed zeolites even though the size of these ions is very different. It is believed that the role of the alkali ions is to compensate the charges from a large number of the framework defects ($\equiv\text{Si}-\text{O}^-\dots\text{H}-\text{O}-\text{Si}\equiv$) caused by the relatively high charge/volume ratio of TEA^+ . The observation is consistent with the previous studies on the formation of high silica zeolite BEA in the presence of TEA^+ and Na^+ .^{35, 39}

Fig. 3(a) reveals the XRD patterns of as-made Sn-BEA (Sn-BEA-AM), Sn-BEA after direct calcination (Sn-BEA-DC) and Sn-BEA after ion-exchange and calcination (Sn-BEA-IE). Sn-BEA-AM shows typical diffraction peaks corresponding to zeolite BEA phase. However, much weaker peaks are observed in the XRD pattern of Sn-BEA-DC which is made by direct

calcination without ion-exchange, indicating the crystalline structure of the sample was significantly damaged. The partial collapse of crystalline structure during calcination might be attributed to the inherent defects ($\equiv\text{SiO}^-$) generated for compensating the positive charges from the TEA^+ ions.

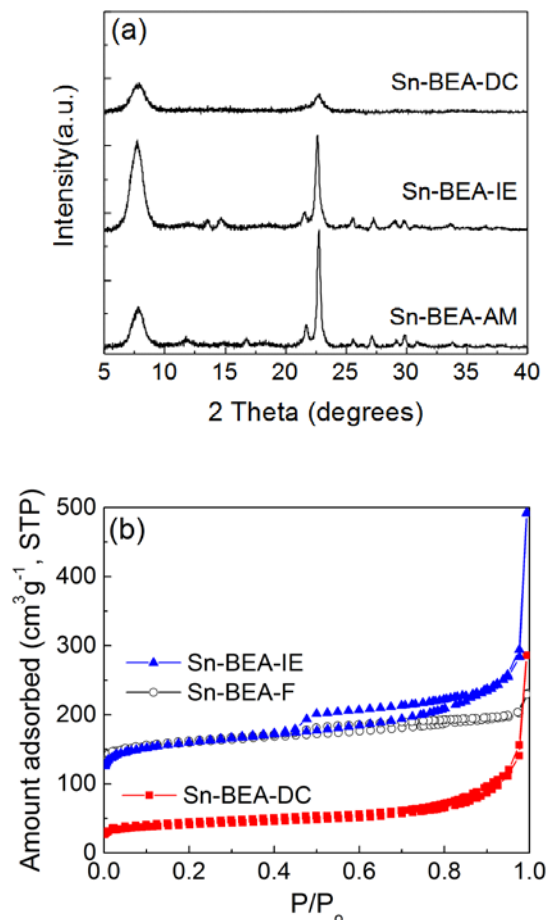


Fig. 3 (a) XRD patterns of Sn-BEA-AM, Sn-BEA-IE, and Sn-BEA-DC and (b) nitrogen sorption isotherms of Sn-BEA-DC, Sn-BEA-IE and Sn-BEA-F.

Because of no aluminum in the zeolite framework, positive charges from the TEA^+ occluded within Sn-BEA samples can generate much more framework defects ($\equiv\text{SiO}^-$) than Al-BEA. Formation of BEA crystalline phase under the conditions thus requires use of alkali ions (*e.g.* Na^+ , K^+ and Li^+) to compensate the additional defects as shown previously. It is interesting that even though crystalline phase can be achieved using Na^+ in the synthesis solution, the $\equiv\text{Si}-\text{O}-\text{Na}$ structure could not undergo condensation with adjacent defect sites ($\equiv\text{Si}-\text{O}-\text{H}$ or $\equiv\text{Si}-\text{O}-\text{Na}$) to form $\equiv\text{Si}-\text{O}-\text{Si}\equiv$ during calcination. As a result, the crystalline structure collapsed after the removal of TEA^+ (Sn-BEA-DC) by calcination. Interestingly, it was found that the crystalline structure can be well retained by the ion-exchange of Na^+ with NH_4^+ before the calcination. Sn-BEA-IE sample made by the ion-exchange of Sn-BEA-AM with ammonium nitrate (NH_4NO_3) solution and subsequent calcination exhibits well-

crystalline BEA structure (Fig. 3(a)). It is believed that the Na^+ and some TEA^+ were replaced by NH_4^+ during the ion-exchange. Upon further heat treatment, $\equiv\text{Si-O-NH}_4$ could be transformed into $\equiv\text{Si-O-H}$. Subsequent dehydration/condensation of the silanol groups could lead to the formation of $\equiv\text{Si-O-Si}\equiv$ bond, which benefits retaining the crystallinity and microporous structure of Sn-BEA (Scheme 1). This result clearly suggests that exchanging alkali ions from the zeolite samples by NH_4^+ is indispensable for obtaining highly crystalline Sn-BEA catalyst under the synthesis route used in this study. The method might also be applicable for retaining the crystallinity of other high silica or siliceous zeolites that have a large number of OSDAs and defects in the as-made forms. It was also attempted to replace the alkali ions (e.g. Na^+ , K^+ , Li^+) by NH_4^+ ion in the synthesis mixture as the charge compensator to avoid the ion-exchange process. However, no crystalline phase was achieved under the synthesis conditions (Fig. S2). The ineffectiveness of NH_4^+ ion for stabilizing zeolite structure during crystallization might be due to the steric hindrance with the TEA^+ ion within zeolite BEA framework.

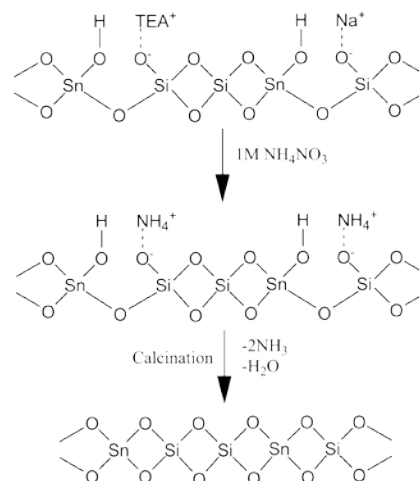
Nitrogen sorption isotherms (Fig. 3(b)) also support the high crystallinity of Sn-BEA-IE sample with a micropore volume (V_{mic}) of $0.177 \text{ cm}^3 \text{ g}^{-1}$ (calculated from t-plot), which is comparable to the Sn-BEA-F prepared from a fluoride medium ($V_{\text{mic}} = 0.185 \text{ cm}^3 \text{ g}^{-1}$). However, the sample after direct calcination, Sn-BEA-DC, possesses only limited accessible micropores ($V_{\text{mic}} = 0.033 \text{ cm}^3 \text{ g}^{-1}$) due to the destruction of zeolite structure. Additionally, the hysteresis loop appearing on the Sn-BEA-IE sample from $P/P_0 \sim 0.5$ - 0.8 indicates the existence of mesopores. It might be due to the surface roughness and/or the voids created from the intergrowth of small crystal domains as shown in the electron microscopic images (Fig. 4). The result is also consistent with the higher external surface area of Sn-BEA-IE sample ($S_{\text{ext}} = 160 \text{ m}^2 \text{ g}^{-1}$; t-plot method) compared with that in Sn-BEA-F ($S_{\text{ext}} = 121 \text{ m}^2 \text{ g}^{-1}$).

Fig. 4 shows the SEM and TEM images of Sn-BEA-IE sample. Discrete truncated bipyramidal crystals with a size of around 400-700 nm can be observed in the sample (Fig. S3). Sn-BEA-F catalyst synthesized from a fluoride medium (Fig. S4) also shows truncated bipyramidal crystals (600 nm to $1 \mu\text{m}$) but with highly intergrown morphology. The images suggest that Sn-BEA-IE consists of more discrete and smaller crystal domains compared with conventional Sn-BEA, which is consistent with its higher surface area obtained from N_2 sorption experiments. In addition, lattice fringes can be clearly observed in the TEM image (Fig. 4(b)), confirming that the sample is a highly crystalline material. Based on the observations above, it is concluded that Sn-BEA-IE features a well-crystalline structure and a large surface area. The elemental analysis shows that Sn-BEA-IE has a Si/Sn ratio of 102.

Characterizations of Sn coordination

A series of characterization techniques were used to study the structures of Sn site in the synthesized Sn-BEA samples. UV-

Vis spectroscopy has been shown to be an effective method to distinguish the coordination environment of Sn in zeolites.^{28, 38, 40} The absorbance at ~ 200 - 210 nm corresponds to tetrahedrally-coordinated Sn (framework Sn), absorbance at $\sim 240 \text{ nm}$ results from extra-framework Sn species, and the band at $\sim 280 \text{ nm}$ is assigned to Sn in tin dioxide.³⁸ Fig. 5 shows the UV-Vis spectra



Scheme 1 Illustrative representation of the effect of NH_4^+ ion-exchange on crystal structure of the final product.

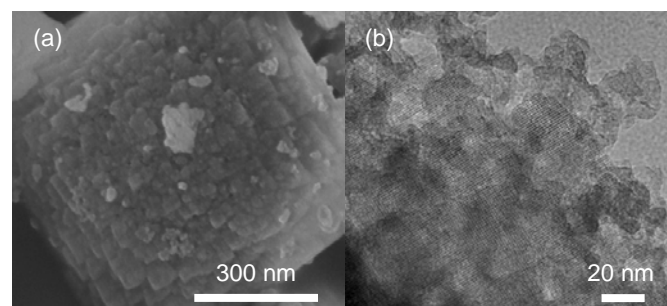


Fig. 4 (a) SEM and (b) TEM images of Sn-BEA-IE synthesized from the DGC method.

for Sn-BEA-IE and Sn-BEA-DC samples. As seen in the plot, the intensified absorbance at $\sim 200 \text{ nm}$ suggests that most Sn in Sn-BEA-IE locate in the framework position (SnO_4 tetrahedral), while there are several different coordination states of Sn observed in Sn-BEA-DC sample. It is plausible that multiple Sn species are formed after zeolite structure collapses during calcination. The result also indicates that the ion-exchange/calcination treatment can preserve the micropore structures of the zeolite samples and the local environment of Sn. The FT-IR spectrum of the Sn-BEA-IE sample with adsorbed pyridine (Fig. 6) reveals that the material exhibits Lewis acidity (1452 cm^{-1}) corresponding to interaction between the isolated Sn sites in the zeolite framework with pyridine.⁹ Moderate Brønsted acidity (1546 cm^{-1}) was also observed in the spectrum, which might originate from the structure defects of the sample ($\equiv\text{Si-OH}$). FT-IR study of CD_3CN adsorption was employed to assess the Lewis acidity of Sn-containing materials.⁴¹⁻⁴³ The CD_3CN adsorbed FT-IR spectra for different

Sn-BEA samples, including Sn-BEA-IE, Sn-BEA-F and SnO₂/Si-BEA, are shown in Fig. 7. The data for Sn-BEA-IE after different desorption times at 100 °C are shown in Fig. 7(a). The band at 2263-2266 cm⁻¹ can be assigned to physically adsorbed CD₃CN, while the band at 2276 cm⁻¹ reflects the interaction of CD₃CN and silanol groups, and the band around 2310 cm⁻¹ is attributed to the vibration related to framework

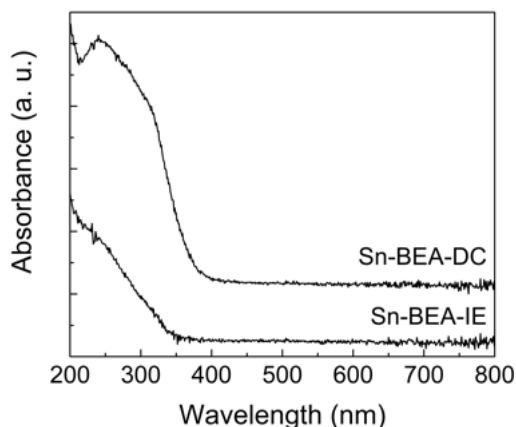


Fig. 5 DR UV-Vis spectra for Sn-BEA-IE and Sn-BEA-DC. The spectrum of Sn-BEA-DC was shifted 0.05 unit for clarity.

Sn species.^{41, 43} It has been proposed that the $\nu(\text{C-N})$ vibrations around 2310 cm⁻¹ can be used to distinguish the “close” (2308 cm⁻¹) or “open” (hydrolyzed; 2316 cm⁻¹) Sn sites in Sn-BEA framework.⁴¹ Interestingly, our data reveal a main band at 2310 cm⁻¹, and no other band at higher wavenumber is observed during the course of CD₃CN desorption, even when desorption temperature was at 150 °C. In contrast, two bands (2308 cm⁻¹ and 2317 cm⁻¹) can be clearly observed during the desorption of CD₃CN for Sn-BEA-F (Fig. 7(b)), which is consistent with previous literature.⁴¹ In addition, the spectra from the sample intentionally made with SnO₂ as extra-framework Sn site did not show absorption at 2305-2317 cm⁻¹ range (SnO₂/Si-BEA, Fig. 7(c); see Fig. S5 for its XRD pattern). These results clearly indicate that the Sn-BEA-IE sample prepared from the DGC method indeed possesses framework Sn, while the local Sn environment could be different from the Sn-BEA-F sample made from fluoride medium. It should be noted that a recent report suggests the two vibration bands can also happen due to the different packing structures of CD₃CN rather than the difference in Sn site structures.⁴³ In addition, the locations and distribution of Sn in zeolite frameworks might also affect their

FT-IR spectra. At this point, it can be concluded that Sn-BEA-IE does have framework Sn site, however the local environment

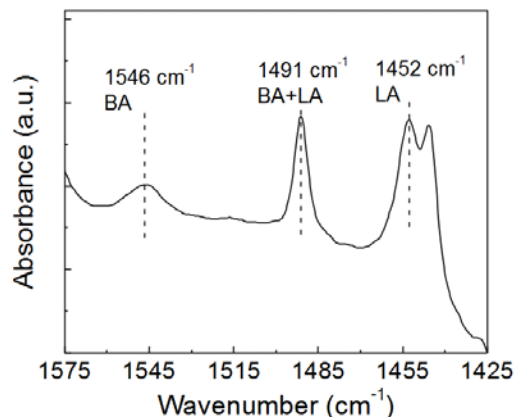


Fig. 6 Pyridine adsorbed FT-IR spectrum of Sn-BEA-IE. BA: Brønsted acid. LA: Lewis acid. The spectrum was acquired after desorbing pyridine at 250 °C for 1h.

of Sn and its difference from the Sn-BEA-F are still elusive, and require further investigation.

To further confirm the coordination environment of Sn in the synthesized Sn-BEA-IE sample, glucose with deuterium substituted at the C-2 position was used in the isomerization reaction.⁴⁴ The ¹H-NMR spectra for unlabelled fructose and fructose isomerized from labelled glucose are shown in Supplementary Information (Fig. S6). The absence of resonances at $\delta = 3.4\text{--}3.5$ ppm corresponding to the protons at C-1 position in ¹H-NMR spectrum of fructose after reaction indicates that the reaction only undergoes an intramolecular hydride shift from C-2 to C-1 in water, which follows the same mechanism as the Sn-BEA-F.⁴⁴ The finding from ¹H-NMR measurement is consistent with the DR UV-Vis and CD₃CN FT-IR measurements, showing most Sn are incorporated into the zeolite framework with a tetrahedral coordination and able to catalyze the glucose isomerization reaction *via* an intramolecular hydride shift pathway. With these characterization results, it is concluded that the Sn-BEA-IE synthesized in this study possesses framework Sn in siliceous BEA framework, and the isolated metal centers exhibit Lewis acidity capable of catalyzing the sugar isomerization in aqueous phase.

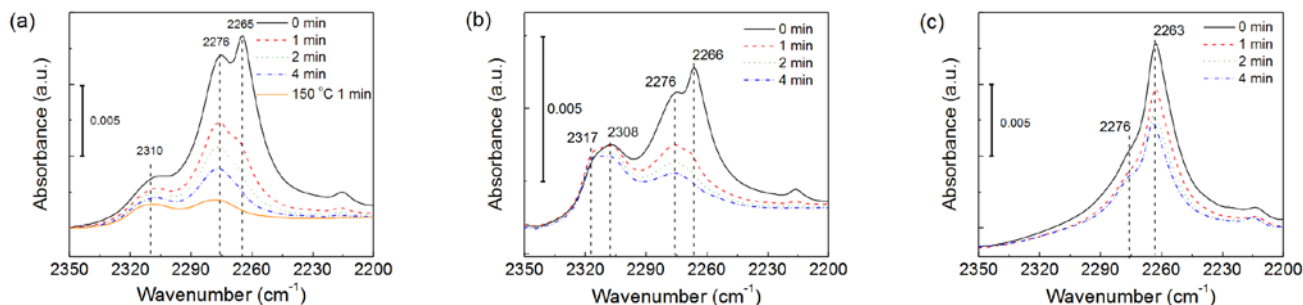


Fig. 7 CD_3CN adsorbed FT-IR spectra of (a) Sn-BEA-IE, (b) Sn-BEA-F and (c) $\text{SnO}_2/\text{Si-BEA}$. The spectra were acquired after saturation of CD_3CN on the samples followed by different period desorption time at $100\text{ }^\circ\text{C}$, as specified in the figures.

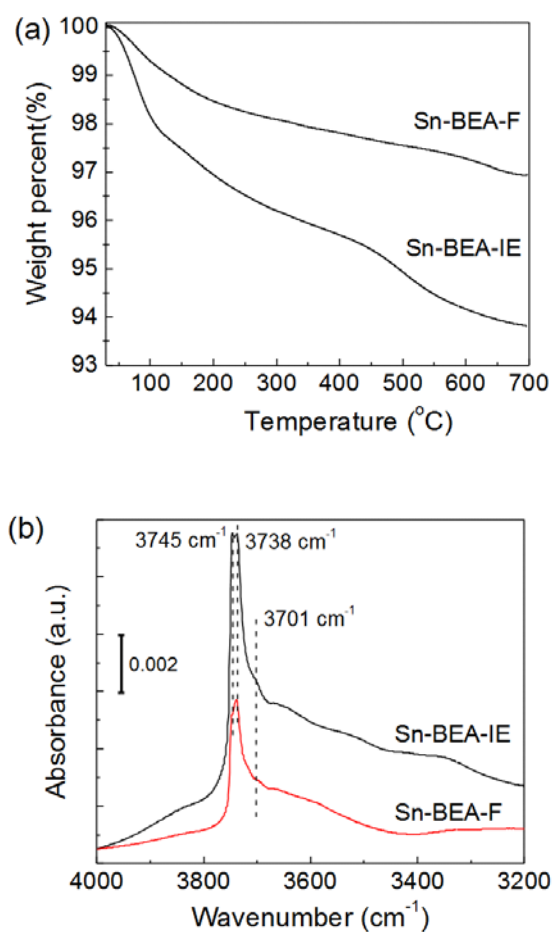


Fig. 8. (a) TGA curves and (b) FT-IR spectra for Sn-BEA-IE and Sn-BEA-F. Samples were contacted with liquid water and dried in a $70\text{ }^\circ\text{C}$ overnight prior to TG measurements. FT-IR spectra were acquired at $30\text{ }^\circ\text{C}$ after degassing at $550\text{ }^\circ\text{C}$ for 1 h. The band at 3745 cm^{-1} represents free terminal silanols, and the bands at 3738 and 3701 cm^{-1} may be related to weakly hydrogen bonded terminal silanols.

Catalytic properties

It has been suggested that the hydrophobic environment is a key factor for adsorbing glucose from aqueous phase into hydrophobic Sn-BEA catalyst and catalyzing the isomerization

reaction from glucose to fructose.^{23, 45, 46} The Sn-BEA catalyst synthesized from the DGC method (Sn-BEA-IE) is expected to have more silanol defects than the sample made from a fluoride medium, and exhibits different hydrophobicity from Sn-BEA-F. This is because the charge of occluded TEA^+ ions in the Sn-BEA-IE synthesized from caustic medium must be compensated by framework defects ($\equiv\text{Si-O}^-$), while in Sn-BEA-F, F^- can form a pair with TEA^+ and generates fewer defects. As discussed in the previous paragraph, the framework defects ($\equiv\text{Si-O}^-$) can be reduced by reacting with adjacent silanol groups in Sn-BEA-IE sample during ion-exchange and calcination processes. However, Sn-BEA-F still has fewer silanol groups ($\equiv\text{Si-OH}$) than Sn-BEA-IE, as shown in a TGA study and FT-IR spectra (Fig. 8). The TG experiments (Fig. 8(a)) clearly suggest that Sn-BEA-IE adsorbs more water (4% vs. 2% weight loss at $400\text{ }^\circ\text{C}$), which implies a more polar surface of Sn-BEA-IE due to the defect structure (Si-OH), and has more hydroxyl condensation at higher temperature ($\sim 2\%$ vs. 0.5% weight loss above $450\text{ }^\circ\text{C}$) than Sn-BEA-F. The FT-IR spectra in the OH stretching region for degassed samples are shown in Fig. 8(b). Intensified absorption bands can be observed at 3738 and 3745 cm^{-1} , which can be assigned to terminal silanol groups (weakly hydrogen bonded and free Si-OH, respectively).⁴⁷ A small shoulder at 3701 cm^{-1} corresponding to weakly hydrogen bonded silanols in zeolites is also observed for Sn-BEA-IE. By directly comparing the normalized spectra, it is obvious that Sn-BEA-IE possesses more silanol groups than Sn-BEA-F does, consistent with TG results. These results indicate that Sn-BEA-IE has more defects and more hydrophilic surface compared to the sample made in the presence of fluoride.^{23, 47}

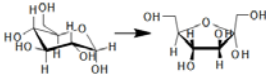
The catalytic activity of the Sn-BEA-IE sample was examined by glucose isomerization and conversion of PA into lactic acid and compared with hydrophobic Sn-BEA-F. The reaction results are summarized in Table 1. The product distributions for different reactions are available in Supplementary Information (Table S1 and S2). As expected, the TOF for the isomerization of glucose into fructose in aqueous phase on Sn-BEA-IE is only $\sim 25\%$ of that of Sn-BEA-F. The low reaction rate is likely due to the hydrophilic surface of Sn-BEA-IE catalyst, which is in good agreement with

previous literature.⁴⁵ On the other hand, the activity of Sn sites in Sn-BEA-IE for the conversion of PA into lactic acid (LA) (1.20 min^{-1}) is still lower than that in Sn-BEA-F (1.52 min^{-1}), but the difference is much less significant compared to the glucose reaction. The production of LA is similar for the two catalysts under the reaction conditions (18.3% vs. 18.9% yield). It has been known that the reaction from PA to LA undergoes hydration of PA in aqueous phase followed by intramolecular 1, 2 hydride-shift reaction on the Lewis acid sites of Sn-BEA.⁸ Hence, it is reasonable that the hydrophilic material shows improved activity due to the enhanced adsorption of water in micropores. However, we must point out that the local environment of Sn sites including “open/close site”, distribution and location might be different for the two Sn-BEA catalysts as revealed in CD_3CN adsorbed FT-IR study which could also affect the catalytic activity of the materials.^{9, 48} Although it is evident that most Sn atoms are incorporated in framework, the discrepancies in activities for different reactions reported here might result from a combinatorial effect of active site nature and surface properties (hydrophobicity).

Conclusions

Highly crystalline Sn-BEA with tetrahedrally coordinated Sn was successfully synthesized from a non-fluoride medium for the first time by a dry gel conversion method. The sample exhibits a higher surface area than the conventional Sn-BEA synthesized from a fluoride medium. It is found that the use of

Table 1 Turnover frequencies (TOF, min^{-1}) of Sn-BEA catalysts for sugar isomerization reactions

Substrate	Reaction Scheme	Sn-BEA-IE	Sn-BEA-F
Pyruvaldehyde ^a		1.20	1.52
Glucose ^b		0.25	0.99

^a 70 °C, 15 min, 20 mg catalyst with 1.06 g 2.1 wt% PA solution

^b 95 °C, 15 min, 68 mg catalyst with 0.80 g 10 wt% glucose solution

seed crystals, addition of alkali ions and ion-exchange with ammonium nitrate before calcination are essential for obtaining a highly crystalline Sn-BEA catalyst. The Sn-BEA catalyst shows lower catalytic activity than the conventional Sn-BEA for glucose isomerization and comparable activity for pyruvaldehyde reaction in aqueous phase. The difference in catalytic activity could be attributed to the different hydrophobic nature and local Sn environment in the catalysts prepared from different synthesis routes. The current work provides an alternative and a more environment-friendly approach to synthesize Sn-BEA catalyst.

Acknowledgements

The authors acknowledge the financial support from Center for Catalysis and Energy Innovation, an Energy Frontier Research Center funded by the U.S. Department of Energy, Office of Science, Office of Basic Energy Sciences under award number DE-SC0001004. We thank Prof. Gonghu Li in University of New Hampshire for his kind help on the DR UV-Vis measurements.

Notes

Department of Chemical Engineering, University of Massachusetts Amherst, 686 North Pleasant St., 159 Goessmann Lab, Amherst, MA 01003, USA. Email: wfan@ecs.umass.edu; Fax: +1-413-545-1647; Tel: +1-413-545-1750.

†Electronic Supplementary Information (ESI) available: the procedures for synthesis of Sn-BEA and $\text{SnO}_2/\text{Si-BEA}$ from a fluoride medium, the XRD patterns for the sample made in the absence of alkali ions and with NH_4^+ salts, SEM image for Sn-BEA-F, XRD pattern for $\text{SnO}_2/\text{Si-BEA}$, product distribution for the reactions and $^1\text{H-NMR}$ spectrum for fructose from the isomerization of deuterium-labeled glucose. See DOI: 10.1039/b000000x/

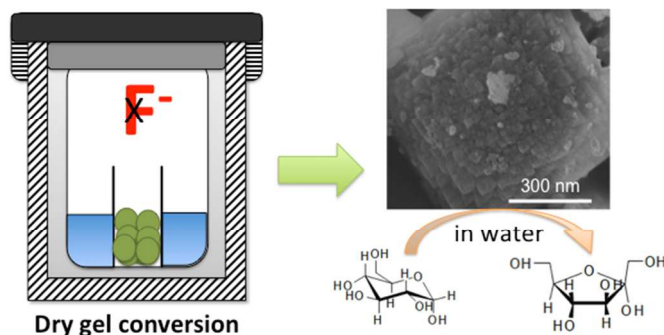
References

- J. Čejka, G. Centi, J. Perez-Pariente and W. J. Roth, *Catal. Today*, 2012, 179, 2-15.
- M. Stöcker, *Angew. Chem., Int. Ed.*, 2008, 47, 9200-9211.
- M. A. Snyder and M. Tsapatsis, *Angew. Chem., Int. Ed.*, 2007, 46, 7560-7573.
- S. G. Wettstein, D. M. Alonso, E. I. Gürbüz and J. A. Dumesic, *Curr. Opin. Chem. Eng.*, 2012, 1, 218-224.
- Y. Zhu, G. Chuah and S. Jaenicke, *Chem. Commun.*, 2003, 2734-2735.
- V. Choudhary, A. B. Pinar, S. I. Sandler, D. G. Vlachos and R. F. Lobo, *ACS Catal.*, 2011, 1, 1724-1728.
- M. Moliner, Y. Román-Leshkov and M. E. Davis, *Proc. Nat. Acad. Sci.*, 2010, 107, 6164-6168.
- E. Taarning, S. Saravanamurugan, M. S. Holm, J. M. Xiong, R. M. West and C. H. Christensen, *ChemSusChem*, 2009, 2, 625-627.
- A. Corma, M. E. Domine and S. Valencia, *J. Catal.*, 2003, 215, 294-304.
- A. Corma, L. T. Nemeth, M. Renz and S. Valencia, *Nature*, 2001, 412, 423-425.
- T. Blasco, M. A. Cambor, A. Corma, P. Esteve, A. Martinez, C. Prieto and S. Valencia, *Chem. Commun.*, 1996, 2367-2368.
- P. Concepción, Y. Pérez, J. C. Hernández-Garrido, M. Fajardo, J. J. Calvino and A. Corma, *Phys. Chem. Chem. Phys.*, 2013, 15, 12048-12055.
- C. Paris, M. Moliner and A. Corma, *Green Chem.*, 2013, 15, 2101-2109.
- C. M. Lew, N. Rajabbeigi and M. Tsapatsis, *Ind. Eng. Chem. Res.*, 2012, 51, 5364-5366.
- E. Nikolla, Y. Román-Leshkov, M. Moliner and M. E. Davis, *ACS Catal.*, 2011, 1, 408-410.
- T. J. Schwartz, S. M. Goodman, C. M. Osmundsen, E. Taarning, M. D. Mozuch, J. Gaskell, D. Cullen, P. J. Kersten and J. A. Dumesic, *ACS Catal.*, 2013, 2689-2693.
- W. R. Gunther, Q. Duong and Y. Román-Leshkov, *J. Mol. Catal. A: Chem.*, 2013, 379, 294-302.
- M. Boronat, P. Concepción, A. Corma and M. Renz, *Catal. Today*, 2007, 121, 39-44.

- 19 A. Corma, M. E. Domine, L. Nemeth and S. Valencia, *J. Am. Chem. Soc.*, 2002, 124, 3194-3195.
- 20 J. N. Chheda, G. W. Huber and J. A. Dumesic, *Angew. Chem., Int. Ed.*, 2007, 46, 7164-7183.
- 21 M. S. Holm, S. Saravanamurugan and E. Taarning, *Science*, 2010, 328, 602-605.
- 22 A. Corma, S. Iborra and A. Velty, *Chem. Rev.*, 2007, 107, 2411-2502.
- 23 R. Gounder and M. E. Davis, *AIChE J.*, 2013, 59, 3349-3358.
- 24 U.S. Patent 5,968,473, 1999.
- 25 Z. Kang, X. Zhang, H. Liu, J. Qiu and K. L. Yeung, *Chem. Eng. J. (Amsterdam, Neth.)*, 2013, 218, 425-432.
- 26 C.-C. Chang, Z. Wang, P. Dornath, H. J. Cho and W. Fan, *RSC Adv.*, 2012, 2, 10475-10477.
- 27 Fluoride: Does-Response Analysis for Non-Cancer Effects, http://water.epa.gov/action/advisories/drinking/fluoride_index.cfm, Accessed February, 2015.
- 28 P. Li, G. Liu, H. Wu, Y. Liu, J.-g. Jiang and P. Wu, *J. Phys. Chem. C*, 2011, 115, 3663-3670.
- 29 C. Hammond, S. Conrad and I. Hermans, *Angew. Chem., Int. Ed.*, 2012, 51, 11736-11739.
- 30 J. Dijkmans, D. Gabriels, M. Dusselier, F. de Clippel, P. Vanelderren, K. Houthoofd, A. Malfliet, Y. Pontikes and B. F. Sels, *Green Chem.*, 2013, 15, 2777-2785.
- 31 A. Corma and M. E. Davis, *ChemPhysChem*, 2004, 5, 304-313.
- 32 F. Vaudry, F. Di Renzo, P. Espiau, F. Fajula and P. Schulz, *Zeolites*, 1997, 19, 253-258.
- 33 V. Shen and A. T. Bell, *Microporous Mater.*, 1996, 7, 187-199.
- 34 W. Xu, J. Dong, J. Li, J. Li and F. Wu, *J. Chem. Soc., Chem. Commun.*, 1990, 755-756.
- 35 P. R. Hari Prasad Rao, K. Ueyama and M. Matsukata, *Appl. Catal., A*, 1998, 166, 97-103.
- 36 X. Ke, L. Xu, C. Zeng, L. Zhang and N. Xu, *Microporous Mesoporous Mater.*, 2007, 106, 68-75.
- 37 M. Ogura, S.-i. Nakata, E. Kikuchi and M. Matsukata, *J. Catal.*, 2001, 199, 41-47.
- 38 R. Bermejo-Deval, R. Gounder and M. E. Davis, *ACS Catal.*, 2012, 2, 2705-2713.
- 39 M. Matsukata, T. Osaki, M. Ogura and E. Kikuchi, *Microporous Mesoporous Mater.*, 2002, 56, 1-10.
- 40 H. Y. Luo, L. Bui, W. R. Gunther, E. Min and Y. Román-Leshkov, *ACS Catal.*, 2012, 2, 2695-2699.
- 41 M. Boronat, P. Concepción, A. Corma, M. Renz and S. Valencia, *J. Catal.*, 2005, 234, 111-118.
- 42 C. M. Osmundsen, M. S. Holm, S. Dahl and E. Taarning, *Proc. R. Soc. A*, 2012, 468, 2000-2016.
- 43 S. Roy, K. Bakhmutsky, E. Mahmoud, R. F. Lobo and R. J. Gorte, *ACS Catal.*, 2013, 3, 573-580.
- 44 Y. Román-Leshkov, M. Moliner, J. A. Labinger and M. E. Davis, *Angew. Chem., Int. Ed.*, 2010, 49, 8954-8957.
- 45 R. Gounder and M. E. Davis, *J. Catal.*, 2013, 308, 176-188.
- 46 C. Buttersack, W. Wach and K. Buchholz, *J. Phys. Chem.*, 1993, 97, 11861-11864.
- 47 T. Blasco, M. A. Camblor, A. Corma, P. Esteve, J. M. Guil, A. Martinez, J. A. Perdigon-Melon and S. Valencia, *J. Phys. Chem. B*, 1998, 102, 75-88.
- 48 G. Yang, E. A. Pidko and E. J. M. Hensen, *J. Phys. Chem. C*, 2013, 117, 3976-3986.

Fluoride-free synthesis of Sn-BEA catalyst by dry gel conversion

Chun-Chih Chang, Hong Je Cho, Zhuopeng Wang, Xuanting Wang and Wei Fan*



Sn-BEA catalyst was synthesized from a fluoride-free medium for the first time *via* a dry gel conversion method. The uses of alkali ions, zeolite BEA seed crystals and ion-exchange before removal of organic template have been shown to be indispensable to obtain the desired material.